International Journal of Advanced Chemistry Research 2025; 7(7): 43-50

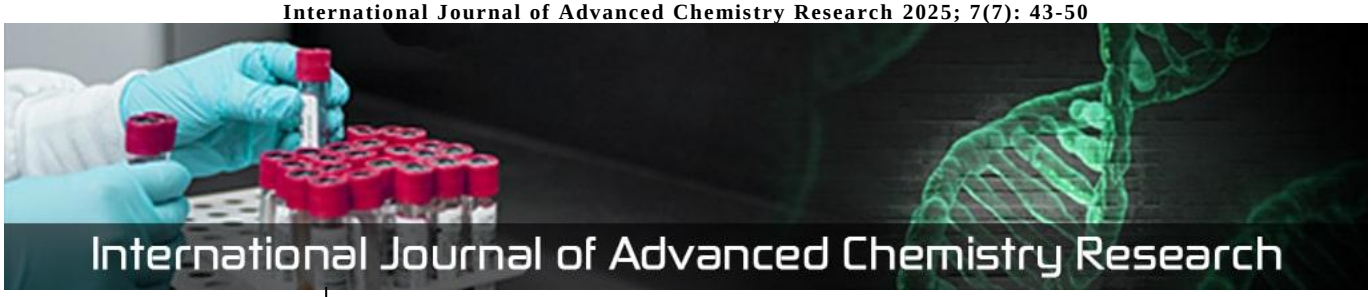

ISSN Print: 2664-6781
ISSN Online: 2664-679X
IJACR 2025; 7(7): 43-50
www.chemistryjournals.net
Received: 17-05-2025
Accepted: 20-06-2025

Subramanian Ravichandran
Department of Physics, Sathyabama of Science and Technology, Jeppiaar Nagar, Chennai, Tamil Nadu, India

Corresponding Author:
Subramanian Ravichandran
Department of Physics, Sathyabama of Science and Technology, Jeppiaar Nagar, Chennai, Tamil Nadu, India

FTIR and acoustical studies of polyacrylamide based alumina oxide nano fluids: Enhancement of physical and thermal properties

Subramanian Ravichandran

DOI: https://www.doi.org/10.33545/26646781.2025.v7.i7a.301

Abstract
Transportation, power generation, micro-manufacturing, electronics, engines, thermal therapy, heating, cooling, ventilation, and air conditioning are just a few of the industrial areas to which nanofluids provide intriguing heat transfer applications. Al_2O_3 nanoparticles have been uniformly suspended in water with varying concentrations in the current work. In the concentration range of 0.1 to 0.8 w/V%, the ultrasonic velocity, absorbance, density, and viscosity measurements were performed. Using a 2 MHz frequency, an ultrasonic interferometer measures ultrasonic velocity and absorption. The conductivity parameter, FTIR properties, viscosity, intermolecular interaction, and molecular free length are used to understand changes in these parameters. As the concentration of alumina oxide increased, the density, viscosity, and sound velocity changed nonlinearly. The drop in molar sound velocity and adiabatic compressibility occurs with concentration, while surface tension, internal pressure, and molecule free length all rise. Different types of molecular contacts, their physico-chemical behavior, and their strength are indicated by variations in acoustic and thermodynamic characteristics.

Keywords: Ultrasonic, velocity-alumina, nanoparticles, acoustical property

Introduction
Nanoparticles are present in nanofluid. Their main use as coolants in heat exchangers and electronic cooling systems is to improve their thermal characteristics. Metallic particles suspended in a considerably smaller volume and size make up nanofluids. Two-phase systems having a single solid phase in a base liquid are called nanofluids [1-4]. Viscosity, heat transfer coefficients, thermal conductivity, and thermal diffusivity are all high in nanofluids. Applications involving heat transfer use nanofluids because of their high thermal conductivity and high heat transfer coefficient. Metal-oxide nanoparticles come in a variety of forms, including nanoscale zinc oxide, titanium oxide, iron oxide, cerium oxide, and zirconium oxide. Specifically, new paint and coating compositions use nano-size pigments and metal-oxides like TiO_2, ZnO, or alumina, cerium, and silica [5-7]. The substance polyacrylamide is an acrylic resin that dissolves especially well in water. Acrylamide undergoes polymerization to produce polyacrylamides. Because of its hydrophilic nature and lack of hazardous effects, polyacrylamide may form extremely high concentrations in aqueous solutions. Water and subsurface applications frequently use polyacrylamide and its derivatives. For water retention, the cross-linked form is commonly utilized. On agricultural land and building sites, the anionic form of linear, water-soluble polyacrylamide is commonly applied as a soil conditioner to stop erosion. High purity aluminium chloride hexhahydrate is used as the raw material in the microwave-assisted sol-gel technique to create alumina nanoparticles. When compared to other nanomaterial synthesis and processing methods, alumina nanoparticles are easier to synthesize and more cost-effective. Alumina nanoparticles in particular are anticipated to be crucial in a number of applications, including electronic substrates, furnace liner tubes, thermometry sensors, gas laser tubes, high temperature electrical insulators, high voltage insulators, and antibacterial properties.
Using ultrasonication, homogenous suspensions of nanosized Al_2O_3 in polyacrylamide were made in different concentrations for the current study [8-10].

Materials and Methods

Sigma Aldrich supplied the high-purity, AR-grade polyacrylamide, ammonium acetate, and aluminium chloride (hexahydrate) were used in this experiment. Demineralized water was used to prepare each solution. In order to minimize evaporation losses, mixtures were produced by weighing the liquids in ground stoppered weighing bottles. An electronic balance (Shimadzu Electronic Balance) with an accuracy of 0.01 mg was used for all weightings. The sol-gel method with microwave assistance was used to carry out the synthesis. Ammonium acetate, aluminium chloride hexahydrate, and a magnetic stirrer were combined at 80° C. At the end of the procedure, a translucent gel was produced, which was scraped off and dried in a microwave. After solidifying, the substance was ground into a powder. To get rid of any remaining water, the resulting powder was crushed, filtered, and baked. Alumina nanoparticles were uniformly prepared in polyacrylamide solution to create nanofluids. Al_2O_3 nanofluid with a concentration of 0.1% to 0.8% (W/V) was created by dispersing the resulting Al_2O_3 nano powder in a polymer solution. In order to determine the viscosity of the suspensions, the fluid flow durations were measured with an accuracy of ±0.2% using Ostwald's viscometer. A specific gravity bottle was used to measure the fluids' densities. The KD2 Pro Thermal Analyzer was used to measure the thermal conductivity at 303 K. After being cooked to the appropriate temperature in a water bath, the sample was left to stabilize. Thermal conductivity was then measured using the thermal analyzer. of the sample of nanofluid was measured. The MHF-400 high frequency pulser receiver was used to evaluate the velocity values of ultrasonic wave propagation through the nanofluid samples in various ratios at frequencies of 2 MHz and 10 MHz at various temperatures. Water from a thermostatically regulated water bath was circulated to maintain the steady temperatures. Density, viscosity, and ultrasonic velocity are used to compute acoustic parameters such adiabatic compressibility, acoustical impedance, intermolecular free length, and surface tension.

Results and Discussion

FTIR Characterization of [Al_2O_3] nanoparticle

Figure 1 displays the synthesized nanoparticle's FTIR spectrum. Al-O-Al stretching vibration is the cause of the vibrational peaks at 646 cm-1. The peaks are attributed to alumina and are located between 400 and 962 cm-1. The vibrational peaks that correlate to the C-O stretching vibration are located at 1082.39 cm-1 and 1166.06 cm-1. Vibrational peaks at 1406.8 cm-1 and 1633.78 cm-1 are attributed to the solvent water's O-H bending vibration. In the 3391.09-2500 cm-1 range, the vibration peaks correspond to the O-H stretching vibration. The shape of the nanoparticles made using the microwave-assisted sol-gel process is revealed by scanning electron microscopy (SEM) analysis. Alumina crystals are shown by the hexagon-shaped structure (Fig. 3). Figure 2's alumina nanoparticle EDX pattern revealed the existence of Al and O

A versatile, non-destructive analytical technique for identifying the crystalline phases of different powder and solid materials is X-ray diffraction. Figure 4 displays the synthesized alumina powder's X-ray pattern. All of the diffraction peaks align with the stated 2θ values and standard patterns of pure alumina's hexagonal structure (JCPDS No. 01-079-0207). The lattice planes (012), (104), (024), and (116) correspond to the diffraction peaks at 2θ, which are 24.7°, 32.4°, 47.18°, and 57.9°. It demonstrates the resulting alumina nanoparticle. It has been determined that the prepared sample Alumina has an average crystalline size of 23.4 nm. The prepared sample's identity as an alumina nanoparticle is confirmed [11-15]. Al_2O_3's density and ultrasonic velocity in a polyacrylamide solution were measured for different concentrations at 303K, and Tables 1-4 provide this information. The change in ultrasonic velocity with varying mole fraction is depicted in Fig. 5. These differences rely on structural alterations brought about by interactions between the solute and solvent molecules. The velocity value drops above the concentration of 0.6%, suggesting that the nanoparticle-fluid interaction is decreasing and the particle-particle interaction is increasing.

The change in adiabatic compressibility with varying mole fraction is depicted in Fig. 6. As the nanoparticle-fluid interaction grows and the particle-particle interaction decreases, the adiabatic compressibility value rises. A greater degree of connection between the solute and solvent molecules is indicated by an increase in adiabatic compressibility at higher concentrations. Ultrasonic velocity has the opposite effect from adiabatic compressibility. The intermolecular free length and acoustical impedance variations are displayed in Figures 7 and 8. As the concentration of nanofluids rises, so do the free length and acoustical impedance. It shows that Brownian motion causes a decrease in the molecular forces of attraction. The square of the ultrasonic velocity has an inverse relationship with adiabatic compressibility. The following factor can be used to characterize the deviation in adiabatic compressibility. 1. The loss of di-polar connection and variations in the size and shape of the constituent molecules result in a drop in velocity and an increase in compressibility. 2. Dipole-dipole interactions or the creation of hydrogen-bonded complex ions result in an increase in ultrasonic velocity and a decrease in adiabatic compressibility. The resulting effect determines the actual deviation [16-17]. The noted significant interaction between the component molecules in the binary mixtures is demonstrated by changes in adiabatic compressibility, intermolecular free length, acoustic impedance, and relative association with composition.

Thermal Conductivity of nanofluids

One of a material's thermal characteristics that allows heat energy to be transmitted is thermal conductivity. It is a crucial characteristic for improving the heat transfer fluid's thermal performance. Brownian motion, the weight proportion of dispersed particles, the size and shape of the material, and the type of base fluids all affect thermal behavior. Thermal conductivity measurements for several polymer nanofluids at varying nanophase material concentrations were made for the current studies, and the results are tabulated in Table 6. When a tiny quantity of nanoparticles is added to a fluid, the conductivity changes significantly.

As sample weight and polymer solution concentration increase, so do the values of thermal conductivity. The thermal conductivity of Al2O3 nanoparticles in ethylene glycol at varying volume concentrations was reported by Esfe *et al.* [21]. When Lee and Choi [22] examined the thermal conductivity of Cu-water in ethylene glycol nanofluids, they found that adding 4% more volume fraction of nanoparticles boosted thermal conductivity by 20%. Wang [23] found that when the volume proportion of Al2O3-water increased by 3%, the thermal conductivity increased by 12%. The current study has tested the high thermal conductivity of nanofluids at various concentrations and has determined that the

concentration of Al2O3 nanoparticles increases the thermal conductivity of nanofluids particles [24-25].

Discussion

At varying concentrations, the thermo-acoustical characteristics of Al2O3-polyacrylamide nanofluids were measured. At room temperature, the density, viscosity, and ultrasonic velocity values are determined. Additional thermal characteristics that are more responsive to intermolecular interactions between the constituent molecules of nanofluids are discovered. The structural changes brought about by the association of polymer chains are demonstrated by the linear variations in viscosity of nanofluids. The viscosity of the nanofluids is influenced by the complexity of the polymer chain. Acoustic impedance and adiabatic compressibility also contribute to these interactions. Variations in the intermolecular forces surrounding the solute and solvent molecules are demonstrated by the constant drops in velocity. This impact is supported by the variations in Lf. The concentration of Al2O3 in nanofluids also causes an increase in thermal conductivity. Al2O3 NP typically exhibits high thermal conductivity and transfer of heat energy as a result of the nanoparticle's brownion motion.

Table 1: Experimental value of density, ultrasonic velocity and viscosity of varying concentration of polymer-nano fluid

Sr. No.	Wt: of Alumina nanoparticles in 100ml of polymer solution (g)	Polymer concentration (g/100 ml)	Mole fraction of PA (X_2)	Density (kg/m^3)	Ultrasonic Velocity (m/s)	Viscosity (10^{-3}) (Pa.s)
1.	0	1	0.1104	924.17	1331.36	26.22
2.	0.1	0.1	0.1109	924.98	1462.52	2.808
3.	0.2	0.2	0.1117	923.88	1578.36	3.501
4.	0.3	0.3	0.1123	924.32	1624.08	4.590
5.	0.4	0.4	0.1129	924.39	1637.68	5.609
6.	0.5	0.5	0.1136	924.50	1656.12	7.158
7.	0.6	0.6	0.1145	924.44	1670.28	8.180
8.	0.7	0.7	1.0000	924.70	1676.32	8.643

Table 2: Calculated values of adiabatic compressiblility, acoustic impedance, inter molecular free length, and effective molecular weight of polymer nanofluid

Sr. No	Adiabatic Compressibility (β_{ad}) ($x10^{10}$)	Acoustic Impedance (Z)	Inter molecular free length(L_f) ($x10^{16}$)	Effective Molecular weight (M_{eff})
1.	4.0241	1622081.6	8.1240	9478.2976
2.	3.9793	1631784.2	8.1452	9520.7446
3.	3.8732	1659318.4	8.1874	9503.7658
4.	3.8022	1681612.8	8.2084	9519.0467
5.	3.7226	1700206.4	8.2503	9520.7446
6.	3.4384	1773299.2	8.4055	9512.2552
7.	3.2458	1829497.6	8.5175	9519.8956
8.	3.2870	1760555.5	8.6281	85000.000

Table 3: Calculated values of free volume, internal pressure, molar sound velocity, surface tension and Relaxation time of polymer nano fluids

Sr. No.	Free volume (V) ($x10^{-18}$)	Internal pressure (π)	Molar sound velocity (R)	Surface tension (s)	Relaxation time (τ) ($x10^{9}$)
1.	3.9325	0.0007408	103.1975	39998.4012	1.5066
2.	2.8660	0.0008207	103.7614	40342.5718	1.8576
3.	1.9338	0.0009407	103.2710	41235.8617	2.3703
4.	1.4461	0.0010410	102.7660	41897.1931	2.8436
5.	1.0188	0.0011704	103.0493	42576.5767	3.5528
6.	0.8807	0.0012334	103.7432	45242.2809	3.7503
7.	0.8448	0.0012539	104.2532	47298.0719	3.7405
8.	0.0140	0.0000547	103.1975	46106.4987	1.1492

Table 4: FTIR spectroscopic analysis of polymer solution with different concentration of nano phase materials.

Functional Groups	Weight of Alumina nano particles in 100ml of polymer solution(g)							
	0	0.1	0.2	0.3	0.4	0.5	0.6	0.7
O-H Water Stretch	Strong	Strong	Strong	Strong	Strong	Strong	Strong	Strong
C≡C Alkyes Stretch	Strong	Medium	Strong	Medium	Strong	Strong	Strong	Strong
N-H Stretch Amide	Medium	Strong	Medium	strong	Medium	Medium	Medium	Medium
C-I Stretch Alkyl halide	Variable	Medium	Variable	Variable	Variable	Variable	Variable	Variable
C-Br Stretch	-	-	Variable	Variable	Variable	-	-	-

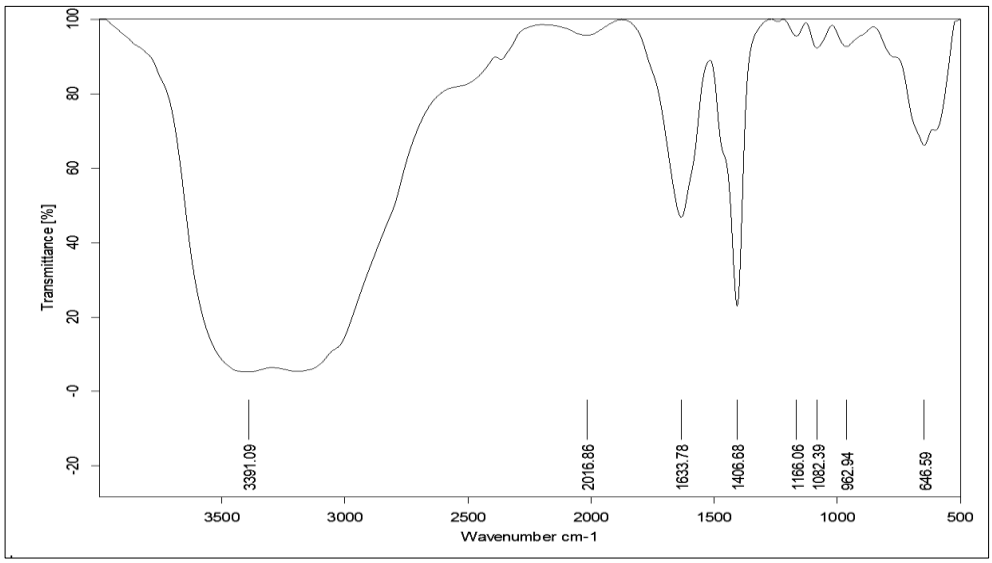

Fig 1: FTIR spectroscopy of alumina nanoparticle

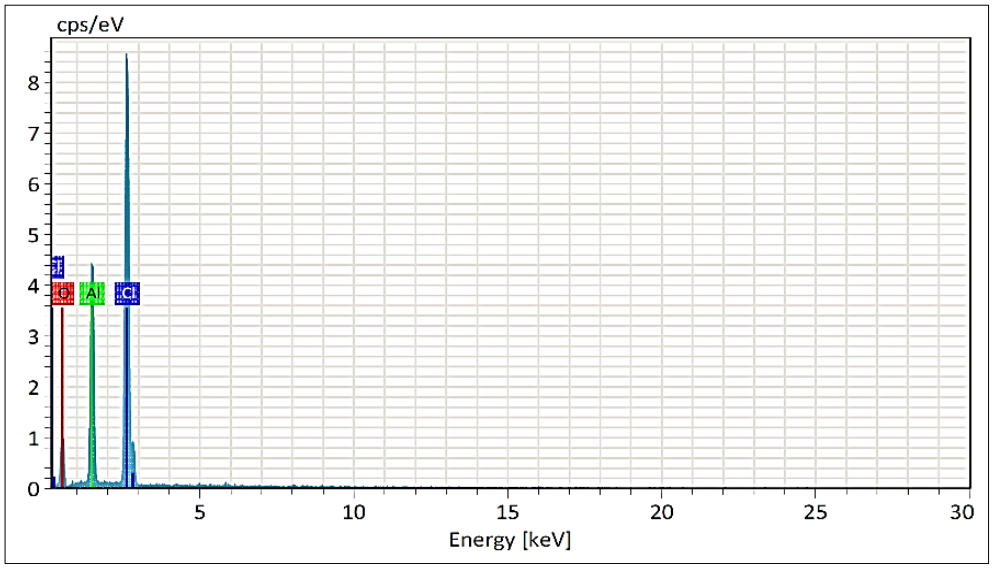

Fig 2: EDX of Alumina nanoparticle

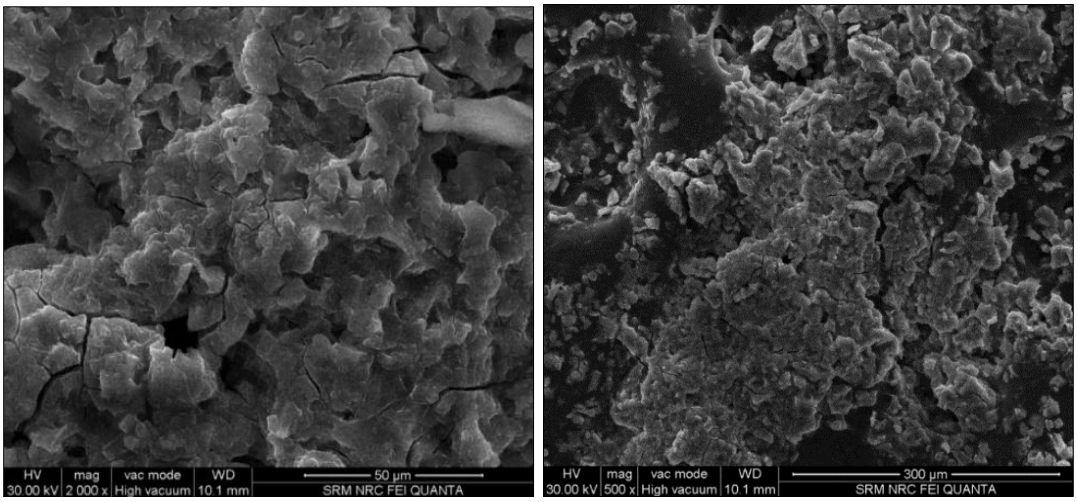

Fig 3: FESEM images of Alumina nanoparticle

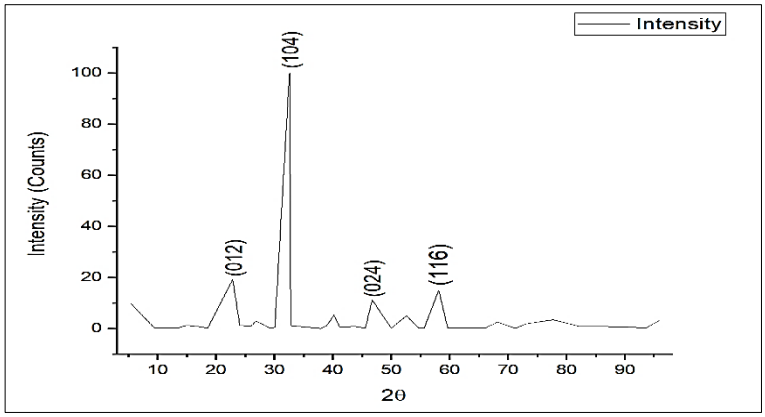

Fig 4: XRD Analysis of Alumina nanoparticle

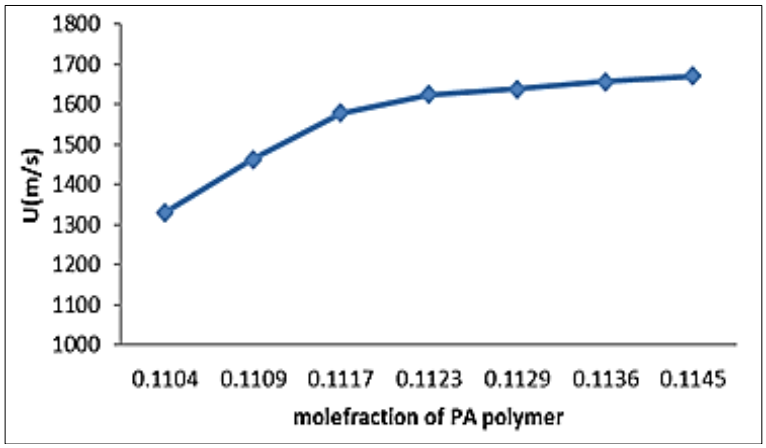

Fig 5: Variation of velocity with mole fraction of PA polymer solution

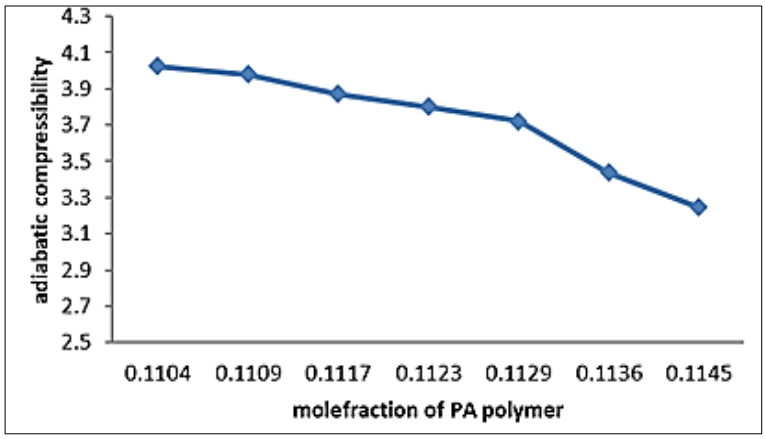

Fig 6: Variation of adiabatic compressibility with mole fraction

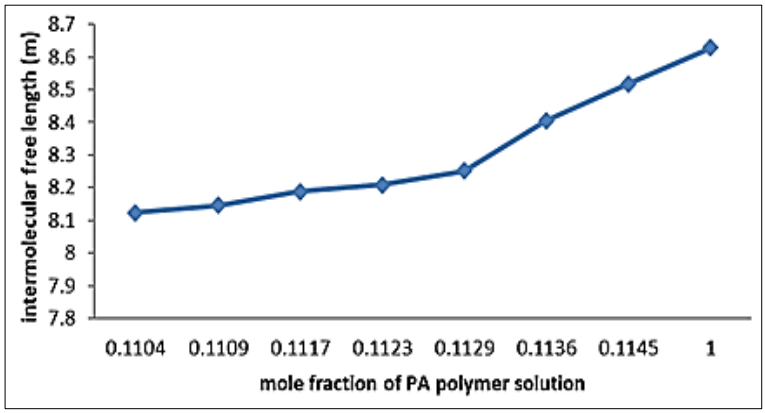

Fig 7: Variation of Inter molecular free length with Concentration of polyacrylamide solution

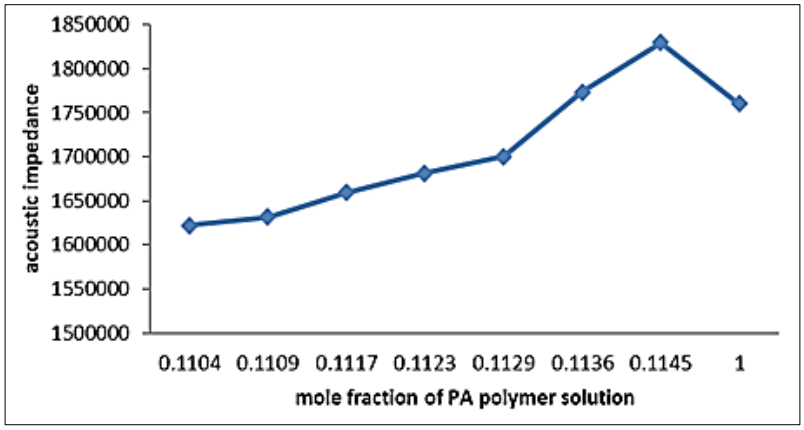

Fig 8: Variation of acoustic impedance with Concentration of polyacrylamide solution

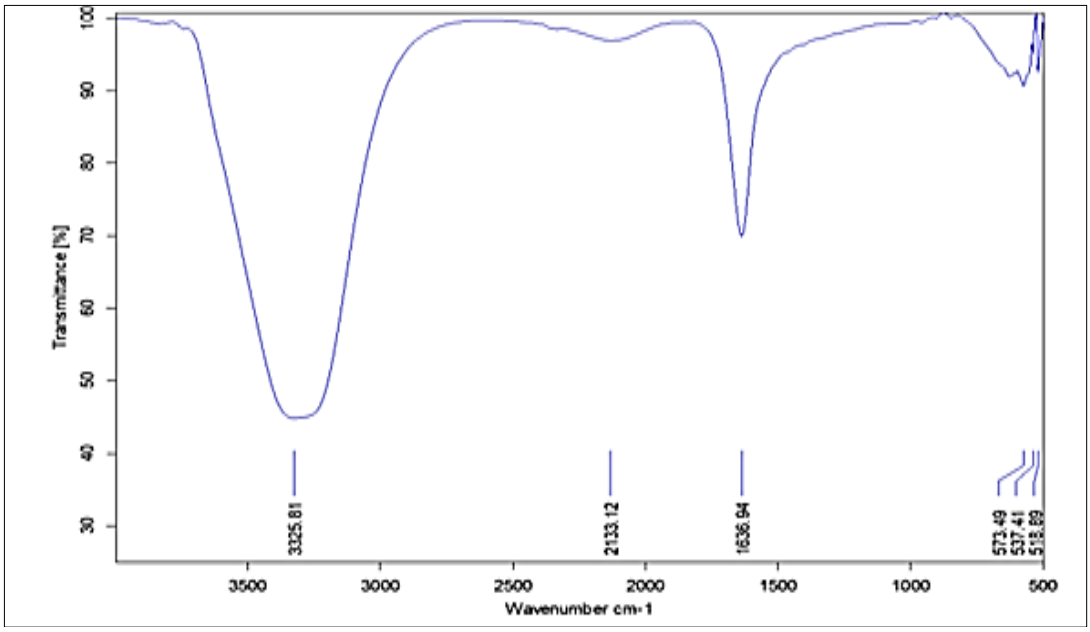

Fig 8.1: FTIR spectrum of 0.1g Alumina nanoparticle

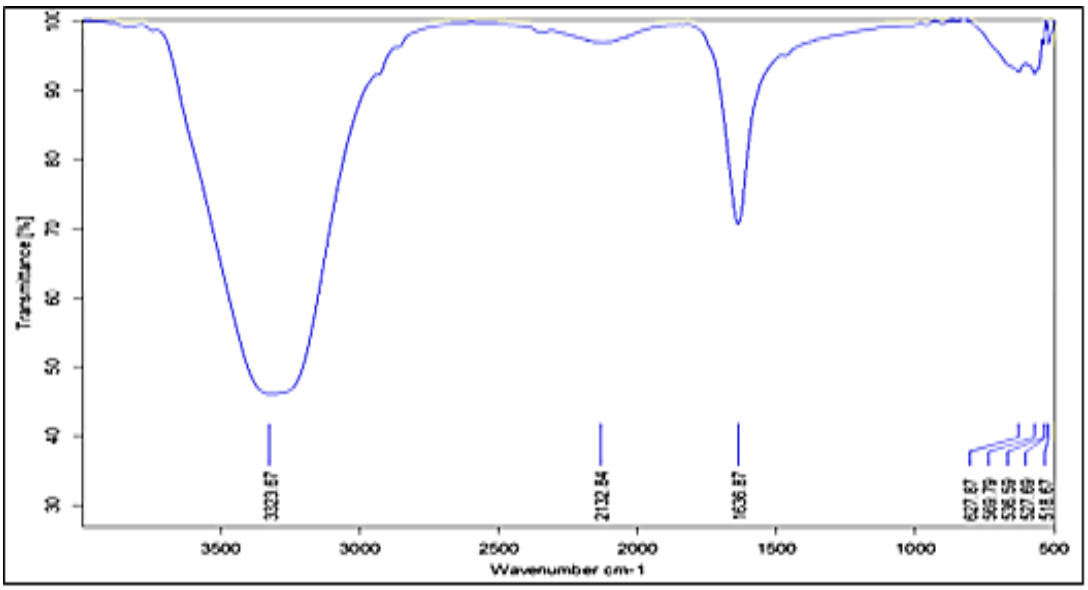

Fig 8.2: FTIR spectrum of 0.2g Alumina nanoparticle in polymer solution in polymer solution

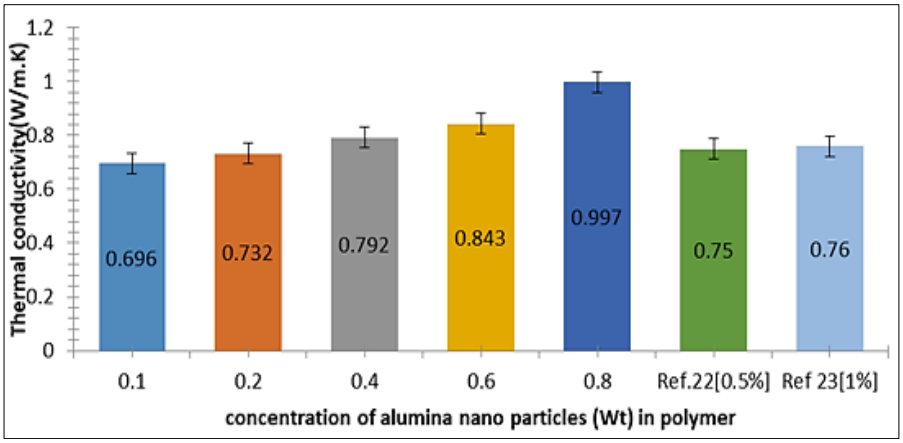

Fig 9: Graph shows the variation of thermal conductivity with different concentration of alumina nano pariticles in polymer solution.

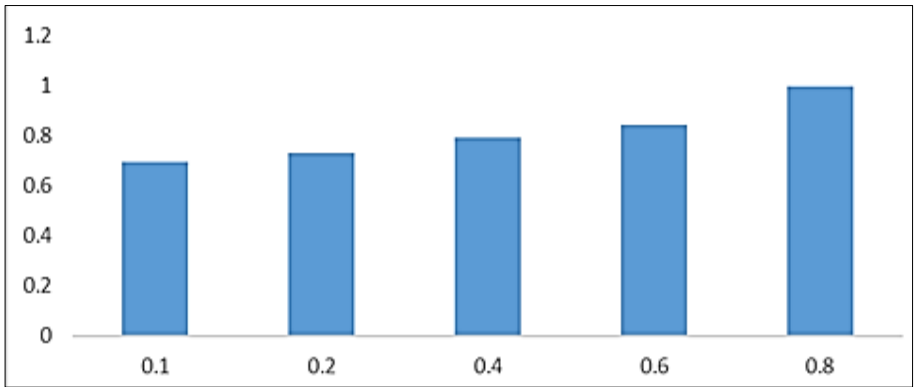

Fig 10: Variation of thermal conductivity with wt of Np-with different concentration of alumina nano pariticles in polymer solution.

Conclusion

As the concentration of the nanocomposite sample increases, the density and viscosity of the nanofluids at different concentrations rise as well. While intermolecular free length and acoustical impedance rise as a result of increased Brownian motion, adiabatic compressibility decreases. The produced solution can be employed for heat transfer applications since the measured thermal conductivity values are higher than those of other alumina composites at 303 K. This is because the heat transfer rate will be higher. As concentration rises, a distinct pattern is detected in the velocity of nanofluids measured as a concentration indicator. As the molar concentration rises, so does the relaxation time. Because it forms hydrogen bonds with the solvent, nanosized alumina has a surface catalytic effect. Additionally, when the alumina nanoparticles and water molecules interact with one another, a hierarchical structure will form, increasing the velocity even more. Therefore, with lower concentrations of nanofluids, the faster velocity of ultrasonic waves is favored by the decrease in compressibility, increase in viscosity, and decrease in density. Thus, it is clear that a strong particle-fluid contact favours velocity growth. The excellent suitability of Al2O3-water fluid for nanofluid applications is known from all the acoustical parameters.

References

1. Shima PD, Philip J. Tuning of thermal conductivity and rheology of nanofluids using an external stimulus. J Phys Chem C. 2011;115:20097-20104.
2. Wang JJ, Zheng RT, Gao JW, Chen G. Heat conduction mechanisms in nanofluids and suspensions. Nano Today. 2012;7:124-136.
3. Turgut A, Tavman I, Chirtoc M, Schuchmann HP, Sauter C, Tavman S. Thermal conductivity and viscosity measurements of water-based TiO_2 nanofluids. Int J Thermophys. 2009;30:1213-1226.
4. Jinklor GT, Bokare JP, Kulkarni TP, Thane MS, Pachore SS, Kabara KB, *et al*. Molecular behaviour of polymer based nanofluids using acoustic method. AIP Conf Proc. 2019;2142:020005.
5. Abdul A, Richard AP, Jacques E. Ultrasonic studies of aqueous solutions of polyvinyl alcohol. Polymer. 1982;23:1446-1450.
6. Eastman JA, Choi SUS, Li S, Yu W, Thompson LJ. Anomalously increased effective thermal conductivities of ethylene glycol-based nanofluids containing copper nanoparticles. Appl Phys Lett. 2001;78:718-721.
7. Choi SUS, Zhang ZG, Yu W, Lockwood FE, Grulke EA. Anomalous thermal conductivity enhancement in nanotube suspensions. Appl Phys Lett. 2001;79:2252-2254.
8. Singh DP, Upmanyu A. Acoustical investigations of molecular interactions in polymer solution of PAN/clay nanocomposites and DMSO. J Polym Biopolym Phys Chem. 2014;2:73-77.
9. Swain SK, Patra SK. Ultrasonic and viscometric study of synthesized PAN/clay nanocomposites. Int J Polym Mater. 2011;60:559-567.
10. Maiti S, Shrivastava N, Suin S, Khatua BB. Low percolation threshold in melt-blended PC/MWCNT nanocomposites in the presence of styrene acrylonitrile (SAN) copolymer: preparation and characterizations. Synth Met. 2013;165:40-46.

11. Nila ASS, Radha KP. Synthesis and XRD, FTIR studies of alumina nanoparticle using co-precipitation method. Int J Res Appl Sci Eng Technol. 2018;6:2321-9653.
12. Rani K, Radha KP, Ananthajothi D. Structural analysis of Cu doped *MgO* nanoparticles using co-precipitation method. Int J Eng Dev Res. 2018;5(4):657-659.
13. Meor Yusoff MS, Muslimin M. Synthesis of alumina using the solvothermal method. Malays J Anal Sci. 2007;11(1):262-268.
14. Afruz FB, Tafreshi MJ. Synthesis of γ-Al_2O_3 nanoparticles by different combustion modes using ammonium carbonate. Indian J Pure Appl Phys. 2014;52:378-385.
15. Selvasekarapanian S, Baskaran R, Kamishima O, Kawamura J, Hattori T. Laser Raman and FTIR studies on Li^+ interaction in PVAc-$LiClO_4$ polymer electrolytes. Spectrochim Acta A Mol Biomol Spectrosc. 2006;65:1234-1240.
16. Jinklor GT, Bokare JP, Kulkarni TP, Thane MS, Pachore SS, Kabara KB, Sarode AV. Molecular behaviour of polymer based nanofluids using acoustic method. AIP Conf Proc. 2019;2142:020005.
17. Nemade KR, Waghuley SA. Room temperature molecular interactions in $CdCl_2/H_2C_2O_4$ nanofluid using acoustical studies. Indian J Pure Appl Phys. 2015;53:670-674.
18. Venu Gopal VR, Kamila S. Thermo-acoustics and rheological properties of various heat transfer fluids blended with *CuO* nanoparticles. BAOJ Nanotechnol. 2016;3(013):1-9.
19. Dash JK, Kamila S. Ion-solvent interactions in lanthanum(III) chloride and D-glucose-water mixed solvent systems: an ultrasonic study. Russ J Phys Chem A. 2015;89(9):1578-1584.
20. Kwak K, Kim C. Viscosity and thermal conductivity of copper oxide nanofluid dispersed in ethylene glycol. Korea-Aust Rheol J. 2005;17(2):35-40.
21. Hemmat Esfe M, Karimipour A, Yan WM, Akbari M, Safaei MR, Dahari M. Experimental study on thermal conductivity of ethylene glycol-based nanofluids containing Al_2O_3 nanoparticles. Int J Heat Mass Transf. 2015;88:728-734.
22. Lee S, Choi SUS. Measuring thermal conductivities of fluids containing oxide nanoparticles. J Heat Transf. 1999;121:280-289.
23. Wang XW, Xu XF, Choi SUS. Thermal conductivity of nanoparticle-fluid mixtures. J Thermophys Heat Transf. 1999;13:474-480.
24. Rashin MN, Hemalatha J. Novel ultrasonic approach to determine thermal conductivity in *CuO*-ethylene glycol nanofluids. J Mol Liq. 2014;197:257-262.
25. Alejandra M, García MJPG, Landa L, Cordero A, Cabañas S, Marcos PMP. Thermal conductivity, rheological behaviour and density of non-Newtonian ethylene glycol-based SnO_2 nanofluids. Fluid Phase Equilib. 2013;337:119-124.
26. Choi SUS. Enhancing thermal conductivity of fluids with nanoparticles. ASME FED. 1995;231:99-103.